Hybrid Control of a Benchmark Cable-Stayed Bridge Considering Nonlinearity of a Lead Rubber Bearing

납고무받침의 비선형성을 고려한 벤치마크 사장교의 복합제어

박 규 식* 정 형 조** 이 인 원***
Park, Kyu Sik Jung, Hyung Jo Lee, In Won

국문요약

본 논문에서는 지진하중을 받는 사장교의 진동제어 기법 개발을 위해 제공된 벤치마크 사장교에 복합제어 기법을 적용하였다. 이 벤치마크 문제는 2003년 완공 예정으로 미국 Missoun 주에 건설중인 Cape Girardeau 교를 대상 구조물로 고려하였다. Cape Girardeau 교는 New Madrid 지진구역에 위치하고 Mississippi 강을 횡단하는 주요 교량이라는 점 때문에 설계 단계에서부터 내진 문제를 중요하게 고려하였다. 벤치마크 문제에는 사장교의 상세한 설계도면에 기초해 교량의 복잡한 거동을 나타낼 수 있는 3차원 선형모델과 각 제어기법의 성능을 평가하기 위한 18개의 평가기준이 제시되어 있다. 본 연구에서 적용한 복합제어 기법은 지진하중으로 인해 구조물에 발생되는 하중을 줄이기 위한 수동제어 기법과 상판변위와 같은 구조물의 응답을 추가적으로 제어하기 위한 능동제어 기법이 결합된 제어 방법이다. 수동제어 장치로는 납고무받침을 사용하였고 Bouc-Wen 모델을 사용하여 비선형 거동을 고려할 수 있도록 모델링 하였다. 능동제어 장치로는 이상적인 hydraulic actuators 가 사용되었으며 제어 알고리듬은 H_2/LQG 를 적용하였다. 수치해석 결과 제안방법의 성능은 수동제어 방법에 비해 매우 효과적이며, 능동제어 방법에 비해서는 약간 좋은 제어 성능을 나타내었다. 복합제어 방법은 수동제어 부분 때문에 능동제어 방법에 비해 보다 신뢰할 수 있는 제어 방법이다. 따라서 제안된 제어방법은 지진하중을 받는 사장교의 제어를 위해 효과적으로 사용될 수 있다.

주요어 : 복합제어 기법, 납고무받침, Bouc-Wen 모델, H_2/LQG 제어 알고리듬, 벤치마크 사장교, 지진응답 제어

ABSTRACT

This paper presents a hybrid control strategy for seismic protection of a benchmark cable-stayed bridge, which is provided as a testbed structure for the development of strategies for the control of cable-stayed bridges. This benchmark problem considers the cable-stayed bridge that is scheduled for completion in Cape Girardeau, Missouri, USA in 2003. Seismic considerations were strongly considered in the design of this bridge due to the location of the bridge in the New Madrid seismic zone and its critical role as a principal crossing of the Mississippi river. Based on detailed drawings of this cable-stayed bridge, a three-dimensional linearlized evaluation model has been developed to represent the complex behavior of the bridge. A set of eighteen evaluation criteria has been developed to evaluate the capabilities of each control strategy. In this study, a hybrid control system is composed of a passive control system to reduce the earthquake-induced forces in the structure and an active control system to further reduce the bridge responses, especially deck displacements. Conventional base isolation devices such as lead rubber bearings are used for the passive control design and Bouc-Wen model is used to simulate the nonlinear behavior of these devices. For the active control design, ideal hydraulic actuators are used and an H_2/LQG control algorithm is adopted. Numerical simulation results show that the performance of the proposed hybrid control strategy is quite effective compared to that of the passive control strategy and slightly better than that of the active control strategy. The hybrid control method is also more reliable than the fully active control method due to the passive control part. Therefore, the proposed hybrid control strategy can effectively be used to seismically excited cable-stayed bridges.

Key words : hybrid control strategy, lead rubber bearing, Bouc-Wen model, H_2/LQG control algorithm, benchmark cable-stayed bridge, seismic response control

1. Introduction

A cable-stayed bridge has become a popular type of bridges throughout the world because of its aesthetic shape, structural efficiency, and economical construction. However, such a structure might be vulnerable to strong earthquake excitations due to its large flexibility and low damping ratios. Structural control systems, such as passive, active, semiactive or a combination thereof, could provide an efficient means for seismic protection of cable-stayed bridges, but the control of such type of bridge is a new, unique and challenging problem because those structures are very flexible.

The main approach to the control of seismically excited cable-stayed bridges that has been used in the past was to isolate the superstructure from the ground excitation by supporting the bridge deck only by the cables[1], which could keep minimum induced seismic forces, resulting in large movements under service loading conditions(i.e., dead and live loads). Therefore, some researchers have considered various connection devices between the deck and the tower in some existing and recently constructed cable-stayed

* 한국과학기술원 건설 및 환경공학과, 박사과정(대표저자 : kyusik@kaist.ac.kr)
** 한국과학기술원 건설 및 환경공학과, 연구조교수
*** 한국과학기술원 건설 및 환경공학과, 교수
본 논문에 대한 토의를 2002년 10월 31일까지 학회로 보내 주시면 그 결과를 게재하겠습니다. (논문접수일 : 2002. 5. 28 / 심사종료일 : 2002. 7. 16)

bridges, such as longitudinal elastic cable restrainer[2], the spring shoes[3], a short pendulum-type link[4], and a vane damper.[5]

Ali and Abdel-Ghaffar[1] investigated a passive control technique by considering the response of bridge models with base isolation devices such as rubber bearings with/without lead plugs. They showed that a significant reduction in earthquake-induced forces could be achieved along the bridge by proper choice of properties and locations of the devices. Iemura et al.[6] investigated the feasibility of structural control technologies for seismic retrofit of a cable-stayed bridge by using rubber bearings and viscous dampers. They verified from numerical simulation of an existing cable-stayed bridge in Japan that the application of structural control strategies in the form of base isolation bearings and dampers is effective in absorbing the large seismic energy and reducing the response amplitudes, consequently seismic demand itself for design.

Under the coordination of the ASCE Committee on Structural Control, Dyke et al.[7] developed the first generation of benchmark structural control problems for seismically excited cable-stayed bridges to investigate the effectiveness of various control strategies. This first generation benchmark control problem considers a bridge currently under construction in Cape Girardeau, Missouri, USA, which will be completed in 2003. This bridge is the Missouri 74-Illinois 146 Bridge spanning the Mississippi River designed by the HNTB Corporation. Seismic considerations were strongly considered in the design of this bridge due to the location of the bridge in the New Madrid seismic zone and its critical role as a principal crossing of the Mississippi River. Based on detailed drawings of this cable-stayed bridge, a three-dimensional linearized evaluation model has been developed to represent the complex behavior of the bridge. For the control design problem, evaluation criteria also have been provided.

In this study, a hybrid control strategy for the seismic protection of a cable-stayed bridge is investigated by using the ASCE first generation benchmark bridge model provided by Dyke et al.[7] The hybrid control strategy is composed of a passive control system to reduce the earthquake-induced forces in the structure and an active control system to further reduce the bridge responses, especially deck displacements. Lead rubber bearings(LRBs) are used for the passive control design and Bouc-Wen model is used to simulate the nonlinear behavior of these devices. For the active control design, ideal hydraulic actuators (HAs) are used and an H_2/LQG control algorithm is adopted. Following a summary of the benchmark problem statement, a seismic control system using the hybrid control strategy is proposed. Then, numerical simulation results are presented to demonstrate the effectiveness of the proposed control strategy.

2. Benchmark problem statement

For completeness, this section briefly summarizes the benchmark cable-stayed bridge problem, including discussion of the bridge model, ground excitations considered, and evaluation criteria, that was developed under the coordination of the ASCE Task Committee on Structural Control Benchmarks. More details can be found in reference (7) and at http://wusceel.cive.wustl.edu/quake/.

This benchmark problem considers the cable-stayed bridge shown in Fig. 1, which is scheduled for completion 2003 in Cape Girardeau, Missouri, USA. In this benchmark study, only the cable-stayed portion of the bridge is considered, because the Illinois approach has a negligible effect on the dynamics of the cable-stayed portion of the bridge.

Based on detailed drawings of the bridge, Dyke et al.[7] developed and made available a three-dimensional linearized evaluation model that effectively represents the complex behavior of the full-scale benchmark bridge. The stiffness matrices used in this linear model are those of the structure determined through a nonlinear static analysis corresponding to the deformed state of the bridge with dead loads. Because this bridge is assumed to be attached to bedrock,

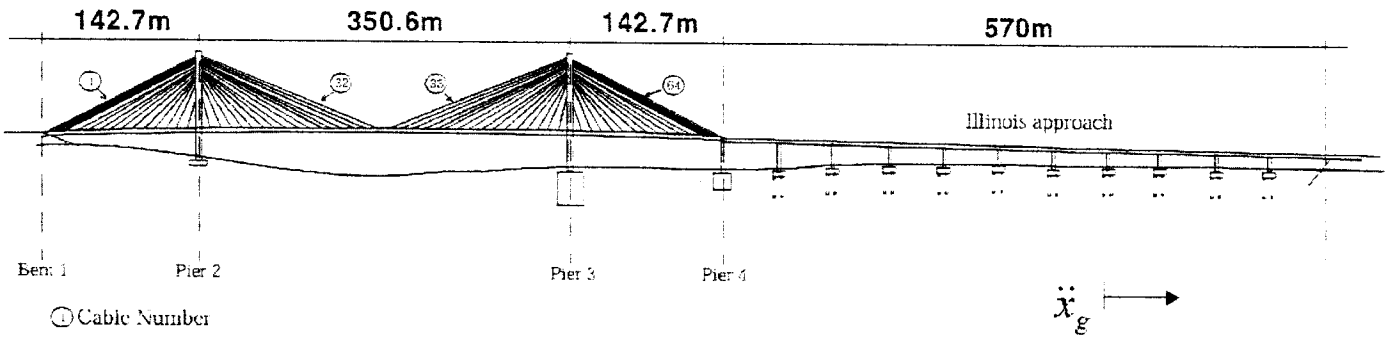

Fig. 1 Schematic of the Cape Girardeau Bridge[7]

the effect of the soil-structure interaction has been neglected. A one-dimensional ground acceleration is applied in the longitudinal direction for this first generation benchmark problem for seismically excited cable-stayed bridges. The bridge model resulting from the finite element formulation, which is modeled by beam elements, cable elements, and rigid links, has a large number of degrees-of-freedom(DOF) and high frequency dynamics. The finite element model of the bridge considered in this study is shown Fig. 2.

Application of static condensation to the full model of the bridge as a model reduction scheme resulted in a 419 DOF reduced-order model, designated the evaluation model. Each mode of this evaluation model has 3% of critical damping, which is consistent with assumptions made during the design of bridge. The first ten frequencies of the evaluation model for the uncontrolled system are 0.2899, 0.3699, 0.4683, 0.5158, 0.5812, 0.6490, 0.6687, 0.6970, 0.7102, and 0.7203Hz. The deck-tower connections in this model are fixed(i.e., the dynamically stiff shock transmission devices are present). On the other hand, another evaluation model should be formed in which the connection between the tower and the deck are disconnected to place control devices acting longitudinally. The first ten frequencies of this second model are 0.1618, 0.2666, 0.3723, 0.4545, 0.5015, 0.5650, 0.6187, 0.6486, 0.6965, and 0.7094 Hz, which are much lower than those of the nominal bridge model.

The following three historical earthquake records are considered as ground excitations for numerical simulations of seismic protective systems installed in the bridge: (1) 1940 El Centro NS, (2) 1985 Mexico City, and (3) 1999 Turkey Gebze NS. The Mexico City earthquake is selected because geological studies have indicated that the Cape Girardeau region is similar to Mexico City. The El Centro and Turkey Gebze earthquakes allow to test proposed control strategies on earthquakes with different characteristics. These three earthquakes are each at or below the design peak ground acceleration level of 0.36g for the bridge. The time-history of the ground acceleration and power spectral density in each earthquake are shown in Fig. 3.

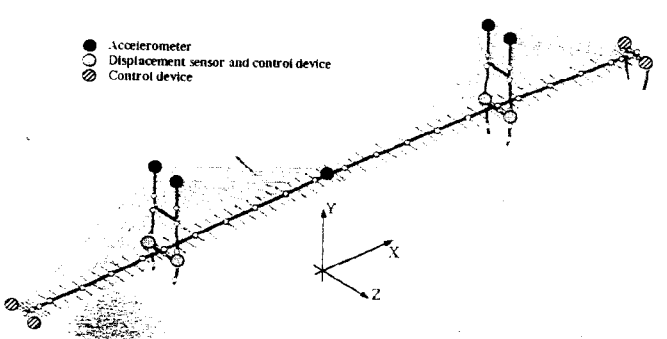

Fig. 2 Finite element model of the Cape Girardeau Bridge and location of sensors and control devices[7]

Eighteen criteria have been defined[7] to evaluate the capabilities of each proposed control strategy. The following first six evaluation criteria considered the ability of the controller to reduce peak response,

$$J_1 = \max_{\substack{ElCentro\\MexicoCity\\Gebze}} \left\{ \frac{\max_{i,t} |F_{bi}(t)|}{F_{0b}^{\max}} \right\},\quad J_2 = \max_{\substack{ElCentro\\MexicoCity\\Gebze}} \left\{ \frac{\max_{i,t} |F_{di}(t)|}{F_{0d}^{\max}} \right\},$$

$$J_3 = \max_{\substack{ElCentro\\MexicoCity\\Gebze}} \left\{ \frac{\max_{i,t} |M_{bi}(t)|}{M_{0b}^{\max}} \right\},\quad J_4 = \max_{\substack{ElCentro\\MexicoCity\\Gebze}} \left\{ \frac{\max_{i,t} |M_{di}(t)|}{M_{0d}^{\max}} \right\},$$

$$J_5 = \max_{\substack{ElCentro\\MexicoCity\\Gebze}} \left\{ \max_{i,t} \left| \frac{T_{ai}(t) - T_{0i}}{T_{0i}} \right| \right\},\quad J_6 = \max_{\substack{ElCentro\\MexicoCity\\Gebze}} \left\{ \max_{i,t} \left| \frac{x_{di}(t)}{x_{0d}} \right| \right\} \tag{1)-(6)}$$

where $F_{bi}(t)$ is the base shear at the ith tower, $F_{0b}^{\max} = \max_{i,t}|F_{0bi}(t)|$ is the maximum uncontrolled base shear, $F_{di}(t)$ is the shear at the deck level in the ith tower, $F_{0d}^{\max} = \max_{i,t}|F_{0di}(t)|$ is the maximum uncontrolled shear at the deck level, $M_{bi}(t)$ is the moment at the base of the tower, $M_{0b}^{\max} = \max_{i,t}|M_{0bi}(t)|$ is the maximum uncontrolled moment at the base of the two towers, $M_{di}(t)$ is the moment at the deck level in the ith tower, $M_{0d}^{\max} = \max_{i,t}|M_{0di}(t)|$ is the maximum uncontrolled moment at the deck level in the two towers, T_{0i} is the nominal pretension in the ith cable, $T_{ai}(t)$ is the actual tension in the cable, $x_{di}(t)$ is the actual deck displacement at bent 1 and pier 4, and x_{0d} is maximum of the uncontrolled deck response at these locations.

The second five evaluation criteria consider normed(i.e., *rms*) responses over the entire simulation time as follows,

$$J_7 = \max_{\substack{ElCentro\\MexicoCity\\Gebze}} \left\{ \frac{\max_{i} \|F_{bi}(t)\|}{\|F_{0b}(t)\|} \right\},\quad J_8 = \max_{\substack{ElCentro\\MexicoCity\\Gebze}} \left\{ \frac{\max_{i} \|F_{di}(t)\|}{\|F_{0d}(t)\|} \right\},$$

$$J_9 = \max_{\substack{ElCentro\\MexicoCity\\Gebze}} \left\{ \frac{\max_{i} \|M_{bi}(t)\|}{\|M_{0b}(t)\|} \right\},\quad J_{10} = \max_{\substack{ElCentro\\MexicoCity\\Gebze}} \left\{ \frac{\max_{i} \|M_{di}(t)\|}{\|M_{0d}(t)\|} \right\},$$

$$J_{11} = \max_{\substack{ElCentro\\MexicoCity\\Gebze}} \left\{ \max_{i} \frac{\|T_{ai}(t) - T_{0i}\|}{T_{0i}} \right\} \tag{7)-(11)}$$

where $\|F_{0b}(t)\|$ is the maximum *rms* uncontrolled base shear of the two towers, $\|F_{0d}(t)\|$ is the maximum *rms* uncontrolled shear at the deck level, $\|M_{0b}(t)\|$ is the maximum *rms* uncontrolled overturning moment of the two towers, $\|F_{0d}(t)\|$ is the maximum *rms* uncontrolled moment at the deck level. The normed value of the response, denoted $\|\cdot\|$, is defined as

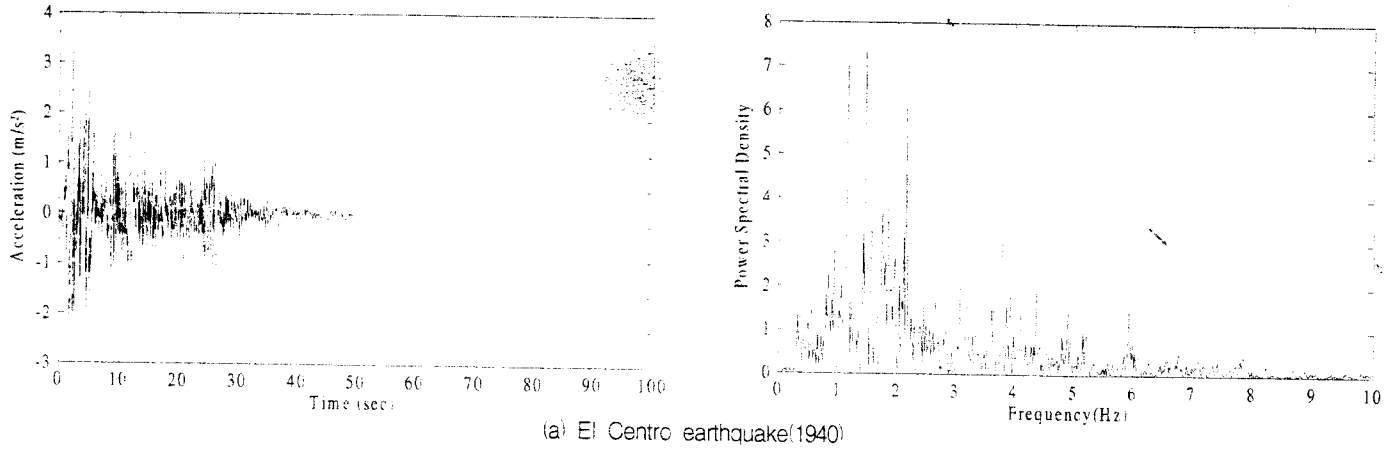

(a) El Centro earthquake(1940)

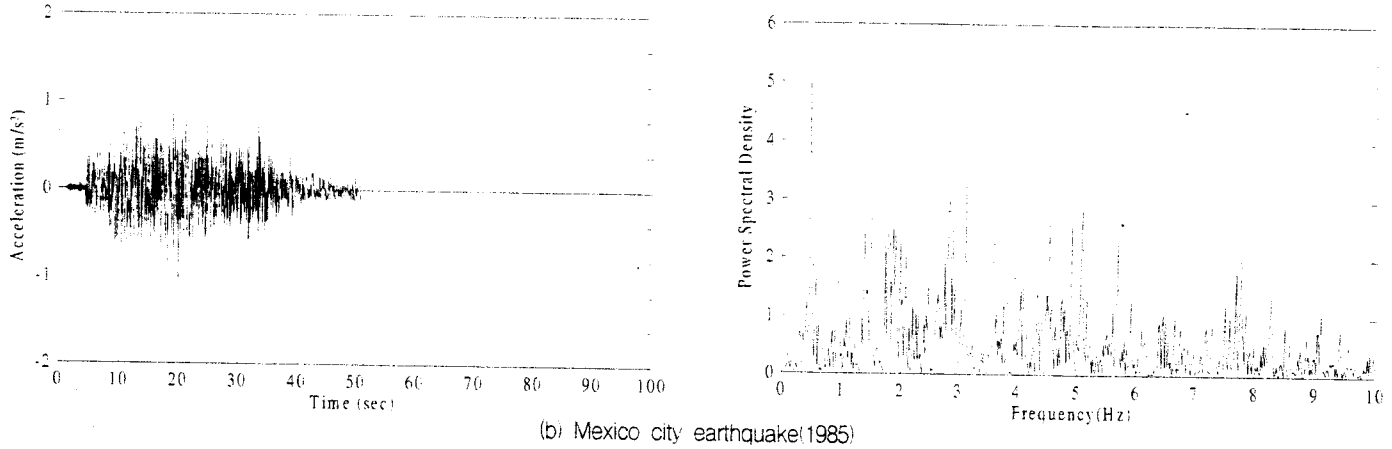

(b) Mexico city earthquake(1985)

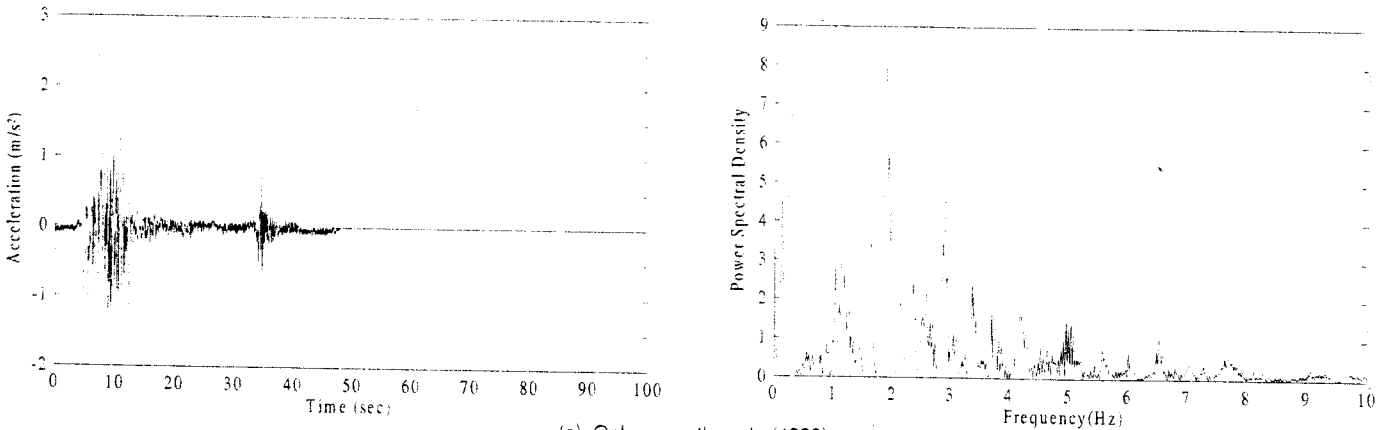

(c) Gebze earthquake(1990)

Fig. 3 Time-history and power spectral density of earthquakes

$$\|\cdot\| = \sqrt{\frac{1}{t_f}\int_0^{t_f}(\cdot)^2 dt} \tag{12}$$

The last seven evaluation criteria consider the requirements of each control system itself,

$$J_{12} = \max_{\substack{\text{ElCentro}\\ \text{MexicoCity}\\ \text{Gebze}}}\left\{\max_{i,t}\left(\frac{f_i(t)}{W}\right)\right\},\quad J_{13} = \max_{\substack{\text{ElCentro}\\ \text{MexicoCity}\\ \text{Gebze}}}\left\{\max_{i,t}\left(\frac{|y_i^d(t)|}{x_0^{\max}}\right)\right\},$$

$$J_{14} = \max_{\substack{\text{ElCentro}\\ \text{MexicoCity}\\ \text{Gebze}}}\left\{\frac{\max_t\left[\sum_i P_i(t)\right]}{\dot{x}_0^{\max}W}\right\},\quad J_{15} = \max_{\substack{\text{ElCentro}\\ \text{MexicoCity}\\ \text{Gebze}}}\left\{\frac{\sum_i\left(\int_0^{t_f} P_i(t)dt\right)}{x_0^{\max}W}\right\},$$

$$\begin{aligned} J_{16} &= \text{number of control devices,}\\ J_{17} &= \text{number of sensors,}\\ J_{18} &= \dim(\mathbf{x}_k^c) \end{aligned} \tag{13)-(19}$$

where $f_i(t)$ is the force generated by the ith control device over the time history, W=510,000kN is the seismic weight of a bridge based on the mass of the superstructure, $y_i^d(t)$ is the stroke of the ith control device, $x_0^{\max}$ is the maximum uncontrolled displacement at the top of the towers relative to the ground, $P_i(t)$ is a measure of the instantaneous power required by the ith control device, $\dot{x}_0^{\max}$ is the peak uncontrolled velocity at the top of the towers, and $\mathbf{x}_k^c$ is the discrete-time state vector of the control algorithm.

3. Seismic control system using a hybrid control strategy

The current level of active control devices was not ready to immediately apply to disaster mitigation strategies for severe earthquakes.[8] To enhance the safety of structures against severe earthquake, more advanced active control strategies with the principle of less energy and better performance should be urgently developed. On the other hand, the hybrid control system can operate well due to the passive control part even if the active control part may not work. Therefore, the hybrid system is more reliable and effective than the passive or active control method alone. In this section, a description of the proposed hybrid control strategy is provided. Bouc-Wen model[9] is used to consider the nonlinear behavior of passive control devices, i.e., LRBs and HAs are used for the active control part of hybrid control strategy and an H_2/LQG control algorithm[10),(11)], which was used for sample controller in the benchmark study, is employed.

3.1 Control devices

3.1.1 Passive control devices

In the hybrid control strategy, passive devices have a great role for the effectiveness of the control method. In this study, conventional base isolation devices such as LRBs are used. The bearings fabricated using rubber and lead offer a simple method of passive control and are relatively easy and inexpensive to manufacture. The design of passive control device follows a general and recommended procedure.[1] In the design procedure, the design shear force level for the yielding of lead plugs is taken to be 0.10M, where M is the part of the deck weight carried by bearings. The asymptotic(or plastic) stiffness ratio of the bearings at the bent and tower are assumed to be 1.0. As the results, a total of 24 LRBs are placed between the deck and pier/bent. Six LRBs are installed between the each deck and pier/bent. The properties of LRBs are shown in Table 1 and these LRBs are installed after removing the horizontal stiffness of beam element in pier 4. Nonlinear model proposed by Wen[9] is used to simulate the motion of nonlinear dynamics. The model has been used for the control simulation in many works.[12)-(15)] The restoring force of the model is composed of the linear and the nonlinear terms as

$$F_{LRB}(x_r, \dot{x}_r) = \alpha k_0 x_r + (1-\alpha) k_0 D_y y \qquad (20)$$

Table 1 The properties of LRB

Property	Value
Elastic stiffness, k_e(N/m)	3.571×10^7
Plastic stiffness, k_p(N/m)	3.139×10^6
Yield displacement of lead plugs, D_y(cm)	0.765
Design shear force level for the yielding of lead plugs, Q_d(kg)	2.540×10^4

where k_0 and α are the linear stiffness and its contribution to restoring force, x_r and $\dot{x}_r$ are relative displacement and relative velocity of nodes which LRBs are installed, respectively. And D_y and y are the yield displacement of LRB and the variable, respectively, satisfying the following equation,

$$\dot{y} = \frac{1}{D_y}\left(A_i \dot{x}_r - \gamma |\dot{x}_r||y|^{n-1} y - \beta \dot{x}_r |y|^n\right) \qquad (21)$$

where A_i, γ, β and n are the constant that affect the hysteretic behavior. The values of $A_i = n = 1$ and $\alpha = \beta = 0.5$ are used to simulate the characteristic curve of the LRB in this study.

3.1.2 Active control devices

In this study, a total of 24 HAs, which are used in the benchmark problem, are employed.[7] Eight between the deck and pier 2, eight between the deck and pier 3, four between the deck and bent 1, and four between the deck and pier 4. The actuators have a capacity of 1000kN. Actuator dynamics are neglected and the actuator is considered to be ideal. The equations describing the forces produced by the actuators are

$$\mathbf{f} = \mathbf{K}_f \mathbf{u} = \mathbf{G}_{dev} \mathbf{D}_d \mathbf{u} = \begin{bmatrix} 2\mathbf{I}_{2\times 2} & \mathbf{0} & \mathbf{0} \\ \mathbf{0} & 4\mathbf{I}_{4\times 4} & \mathbf{0} \\ \mathbf{0} & \mathbf{0} & 2\mathbf{I}_{2\times 2} \end{bmatrix} \mathbf{D}_d \mathbf{u} \qquad (22)$$

$$\mathbf{y}_f = \mathbf{D}_d \mathbf{u} = D_d \mathbf{I}_{8\times 8} \mathbf{u} \qquad (23)$$

where $\mathbf{f}$ is the force output of devices applied to the structure, $\mathbf{y}_f$ is the force output of devices used for feedback in the control algorithm, $D_d = 100\,\mathrm{kN/V}$ is the device gain, and $\mathbf{K}_f$ is a matrix that accounts for the gain of the relationship between the input voltage and the desired control force, as well as the fact that multiple actuators are used at each actuator location, as shown in Eq. (22).

Five accelerometers and four displacement sensors are employed as shown Fig. 2. Four accelerometers are located

on top of the tower legs, and one is located on the deck at mid span. Two displacement sensors are positioned between the deck and pier 2 and two displacement sensors are located between the deck and pier 3. All sensor measurements are obtained in the longitudinal direction to the bridge and are assumed to be ideal, having a constant magnitude and phase.[7] The sensors can be modeled as

$$\mathbf{y}_s = \mathbf{D}_s \mathbf{y}_m + \mathbf{v} \tag{24}$$

where $\mathbf{y}_s$ is a vector of the measured absolute accelerations and device displacements in volts, $\mathbf{y}_m$ is the vector of measured continuous-time absolute accelerations and device displacement in physical units, and $\mathbf{v}$ is the measurement noise, which has an *rms* value of 0.003V. Sensor gain matrix $\mathbf{D}_s$ is

$$\mathbf{D}_s = \begin{bmatrix} \mathbf{I}_{5\times5} G_a & \mathbf{0} \\ \mathbf{0} & \mathbf{I}_{4\times4} G_d \end{bmatrix} \tag{25}$$

where $G_a = 0.714\,\mathrm{V/(m/sec^2)}$ is the sensor gain for acceleration and $G_d = 30\mathrm{V/m}$ is the displacement sensor gain.

3.2 Control design model

A reduced order model of the system is developed for control design, which is formed from the evaluation model and has 30 states. This model obtained by forming a balanced realization of the system and condensing out the states with relatively small controllability and observability grammians.[16] The resulting state space system is represented as follows

$$\dot{\mathbf{x}}_d = \mathbf{A}_d \mathbf{x}_d + \mathbf{B}_d \mathbf{u} + \mathbf{E}_d \ddot{x}_g \tag{26}$$

$$\mathbf{z} = \mathbf{C}_d^z \mathbf{x}_d + \mathbf{D}_d^z \mathbf{u} + \mathbf{F}_d^z \ddot{x}_g \tag{27}$$

$$\mathbf{y}_s = \mathbf{D}_s (\mathbf{C}_d^y \mathbf{x}_d + \mathbf{D}_d^y \mathbf{u} + \mathbf{F}_d^y \ddot{x}_g) + \mathbf{v} \tag{28}$$

where $\mathbf{x}_d$ is the design state vector, $\ddot{x}_g$ is the ground acceleration, $\mathbf{u}$ is the control command input, and $\mathbf{z}$ is the regulated output vector including evaluation outputs(i.e., shear force and moments in the tower, deck displacements, and cable tension forces, etc).

3.3 Control algorithm

In this study, an H_2/LQG control design is adopted for the active control part. For this design, $\ddot{x}_g$ is taken to be a stationary white noise, and an infinite horizontal cost function is chosen as

$$J = \lim_{\tau\to\infty} \frac{1}{\tau} \mathrm{E}\left[\int_0^\tau \left\{ \mathbf{z}^\mathrm{T} \mathbf{Q} \mathbf{z} + \mathbf{u}^\mathrm{T} \mathbf{R} \mathbf{u} \right\} dt \right] \tag{29}$$

where $\mathbf{R}$ is an identity matrix of order 8, and $\mathbf{Q}$ is the response weighting matrix. Further, the measurement noise is assumed to be identically distributed, statistically independent Gaussian white noise process, and $S_{\ddot{x}_g \ddot{x}_g} / S_{v_i v_i} = \gamma = 25$.

In the optimal control such as LQG, obtaining the appropriate weighting parameters is very important to get well-performed controllers. In this study, the maximum response approach is used as follows: i) select the responses which could be considered as the important responses for the overall behaviors of the bridge as shown in Table 2; ii) perform the simulations in each parameter with varying the value of the parameter and determine the appropriate weighting parameters and combination; iii) perform the additional simulation in the combination of the weighting parameters selected in the previous step and finally select the appropriate values of each weighting parameters. This procedure is shown in Figs. 4 and 5. The results are normalized by using those of uncontrolled case(i.e., no devices exist in the connection between deck and pier/bent). As shown in the Fig. 5(a), the overturning moment-weighted and the deck displacement-weighted cases give better reduction of the max. responses than other cases. To select the value of weighting parameters, three-dimensional analysis is conducted as shown Fig. 5(b) with the overturning moment-weighted and deck displacement-weighted parameters.

Consequently, the following combination and values of weighting parameters are obtained through the abovementioned approach for active control system,

$$\mathbf{Q}_{\mathrm{om\_dd}} = \begin{bmatrix} q_{\mathrm{om}} \mathbf{I}_{4\times4} & \mathbf{0} \\ \mathbf{0} & q_{\mathrm{dd}} \mathbf{I}_{4\times4} \end{bmatrix}, \; q_{\mathrm{om}}=4\times10^{-9}, \; q_{\mathrm{dd}}=1\times10^{4} \tag{30}$$

Table 2 The selected responses for optimal weighting parameters

Responses	Corresponding weighting parameters
Base shears at piers 2 and 3	q_{bs}
Shears at deck level at piers 2 and 3	q_{sd}
Overturning moments at base of piers 2 and 3	q_{om}
Moments at deck level at piers 2 and 3	q_{md}
Deck displacements at bent 1 and pier 4	q_{dd}
Top displacements at towers 1 and 2	q_{td}

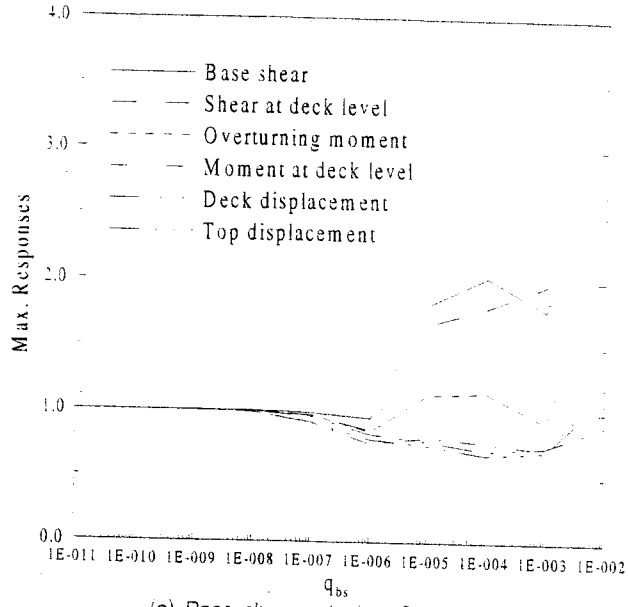

(a) Base shears at piers 2 and 3

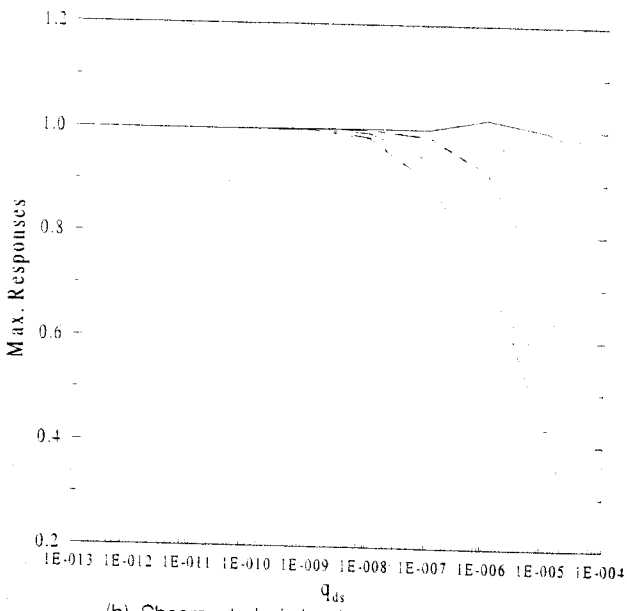

(b) Shears at deck level at piers 2 and 3

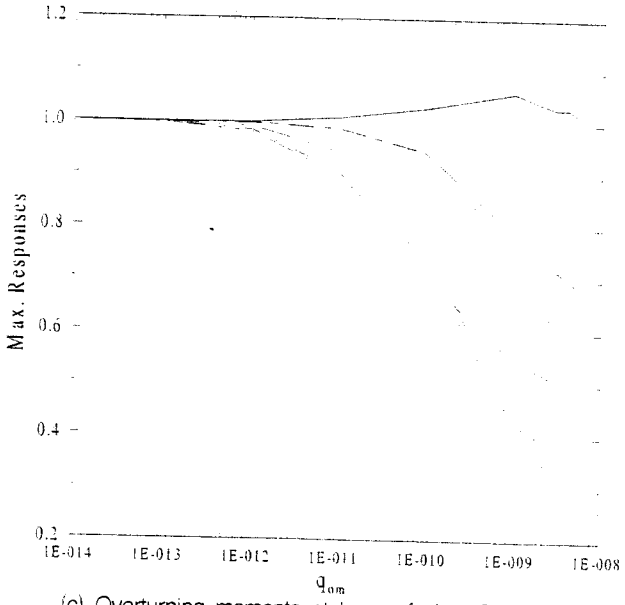

(c) Overturning moments at base of piers 2 and 3

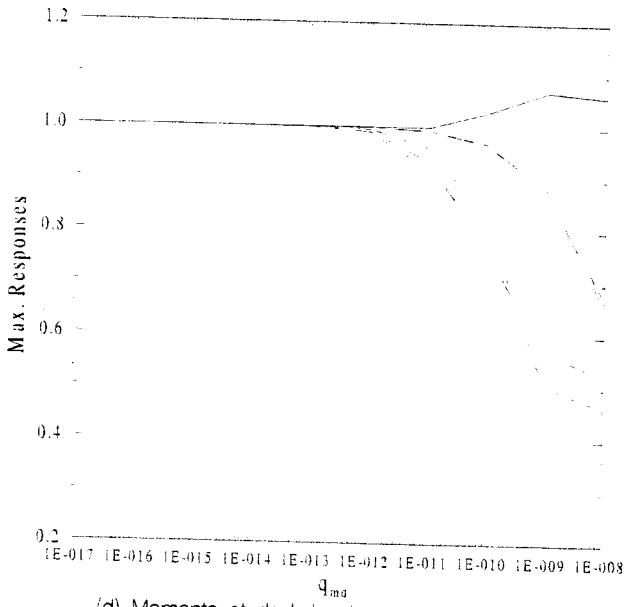

(d) Moments at deck level at piers 2 and 3

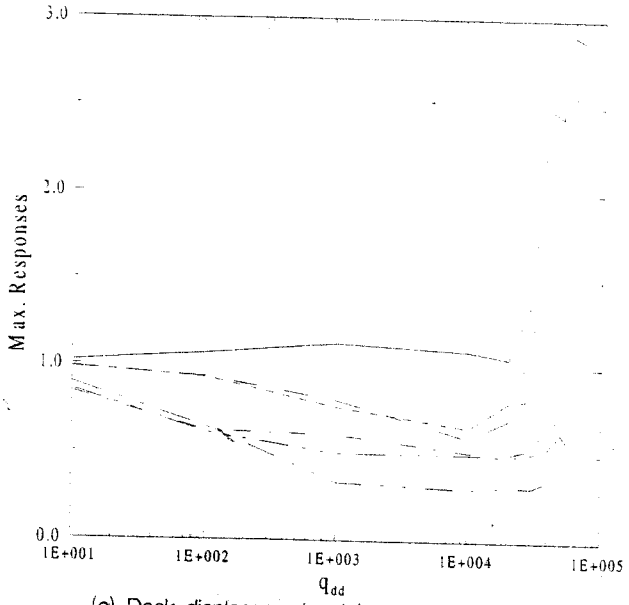

(e) Deck displacements at bent 1 and pier 4

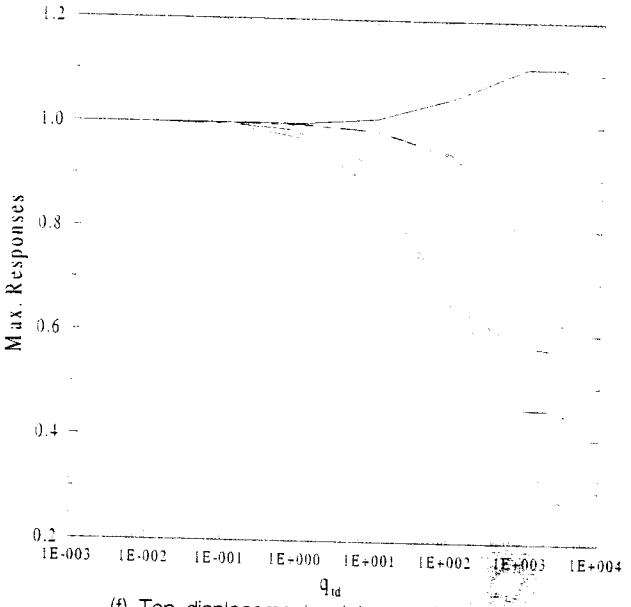

(f) Top displacements at towers 1 and 2

Fig. 4 Weighting parameters vs. max. responses for the active control system

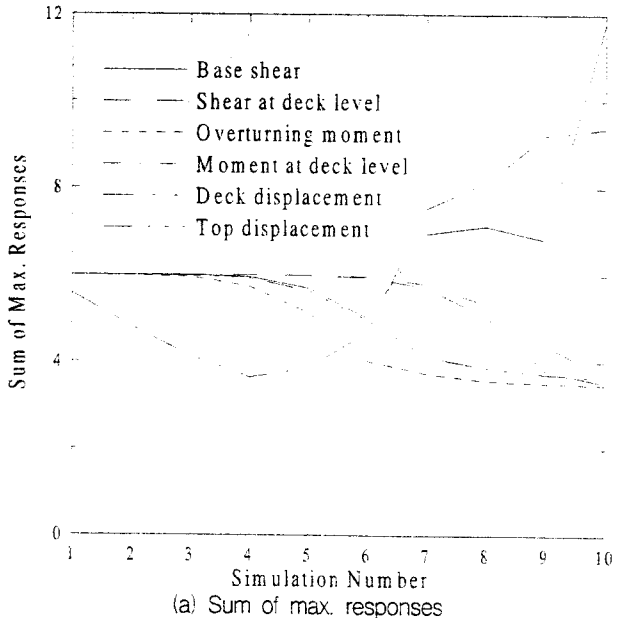

(a) Sum of max. responses

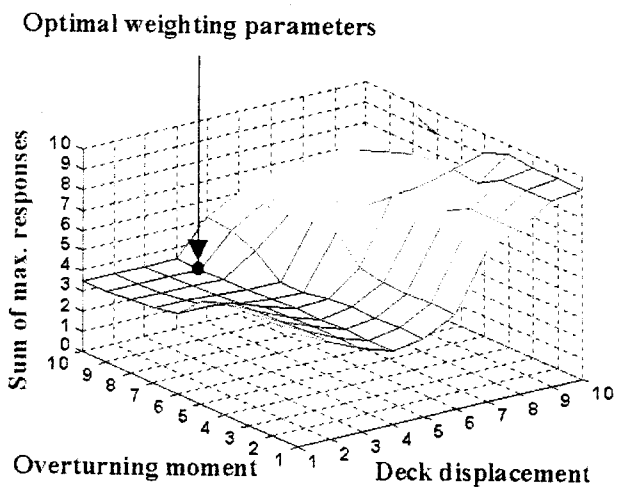

(b) Three dimensional analysis for the selected two weighting parameters

Fig. 5 Selection of appropriate optimal weighting parameters for the active control system

The appropriate weighting parameters of the hybrid control method, which are determined by same procedure as active control strategy is as follows. In Fig. 6, the results are normalized by using those of passive controlled case. The overturning moment- weighted and the deck displacement-weighted cases give better reduction of the max. responses than other cases as shown in Fig 7(a). Therefore, three-dimensional analysis is conducted as shown in Fig. 7(b) similar to the active controlled case.

$$\mathbf{Q}_{om\_dd}=\begin{bmatrix} q_{om}\mathbf{I}_{4\times4} & \mathbf{0} \\ \mathbf{0} & q_{dd}\mathbf{I}_{4\times4} \end{bmatrix},\ q_{om}=5\times10^{-9},\ q_{dd}=1\times10^{5} \qquad (31)$$

4. Numerical simulation results

A set of numerical simulations is performed in MATLAB®[19] for the three historical earthquakes to verify the effectiveness of the hybrid control strategy. Simulation results of the hybrid control design are compared to those of a passive and an active control designs. Tables 3 to 5 show the values of eighteen evaluation criteria for each earthquake. While the controller presented Dyke et al.[7] is not intended to be competitive control design, the associated performance indices are given in these tables for the readers' reference. Table 6 shows the maximum values of eighteen evaluation criteria for all three earthquakes. Viscous damper with the resetting semiactive stiffness damper(RSASD), which is one of the variable stiffness dampers proposed by He et al.[17], is also considered to compare the performance of control strategies. More detailed information on viscous damper with RSASD can be found in He et al.[17]

As seen from the tables, the overall performances of the hybrid control system are superior to those of the passive control system and are slightly better than those of the active control system. The deck displacements of the structure with LRBs are lager than other control strategies. However, the increased deck displacements are still less than the allowable displacement(30cm)[18] and are decreased by additional active devices in the hybrid control method as shown in Fig. 8. Tension in the stay cables remains within a recommended range of allowable values in the considered control strategies.

In the case of the hybrid control system, all the structural responses(J_1~J_4, J_6~J_{10}) are decreased by 14% to 45%(under El Centro earthquake), 11%~24%(under Mexico City earthquake), and 10%~57%(under Gebze earthquake) compared to the passive control system.

The structural responses with the hybrid control system under El Centro earthquake are decreased by 1%~26% compared to the active control system. All the structural responses except the peak shear at deck level(J_2) are decreased by 0.3%~35% under Mexico City earthquake. J_2 is increased by 2%. In the case of Gebze earthquake, the structural responses are decreased by 4%~24%, whereas the normed moment at deck level (J_{10}) is increased by 2%. Fig. 9 shows the uncontrolled and hybrid controlled base shear force record at pier 2.

To demonstrate the feasibility of these controllers, peak values of the force, stroke, and velocity are provided for each earthquake in Table 7. The force, stroke, and velocity

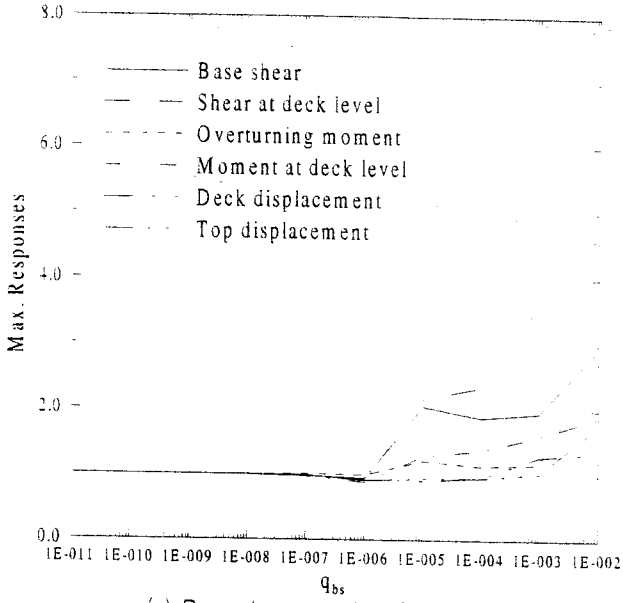

(a) Base shears at piers 2 and 3

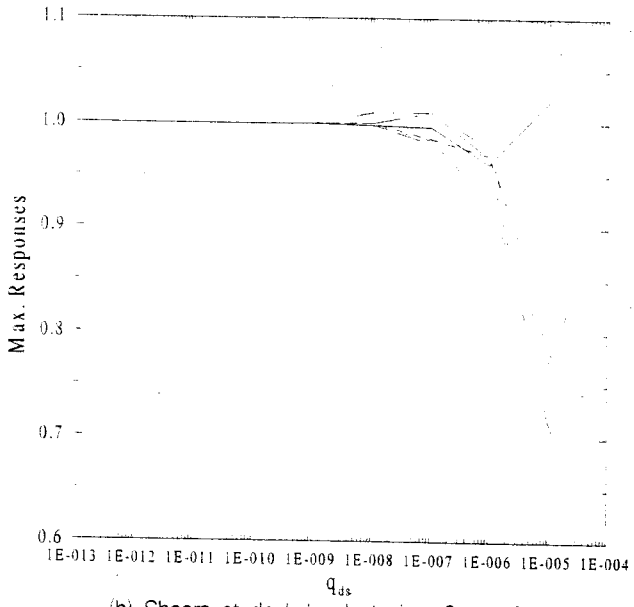

(b) Shears at deck level at piers 2 and 3

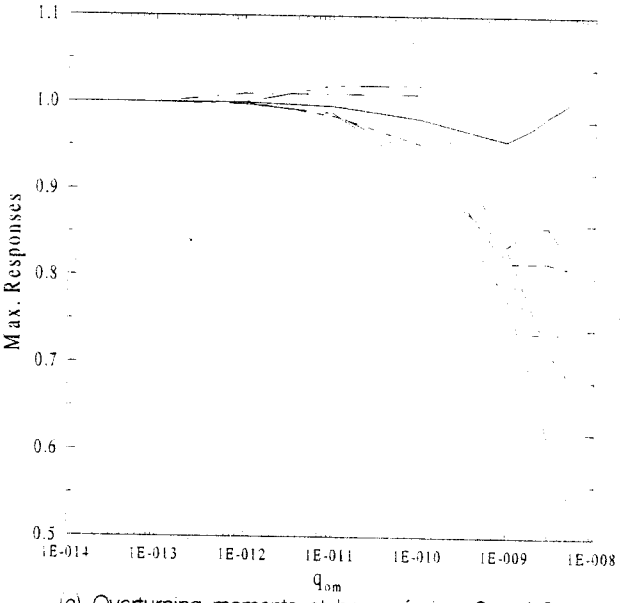

(c) Overturning moments at base of piers 2 and 3

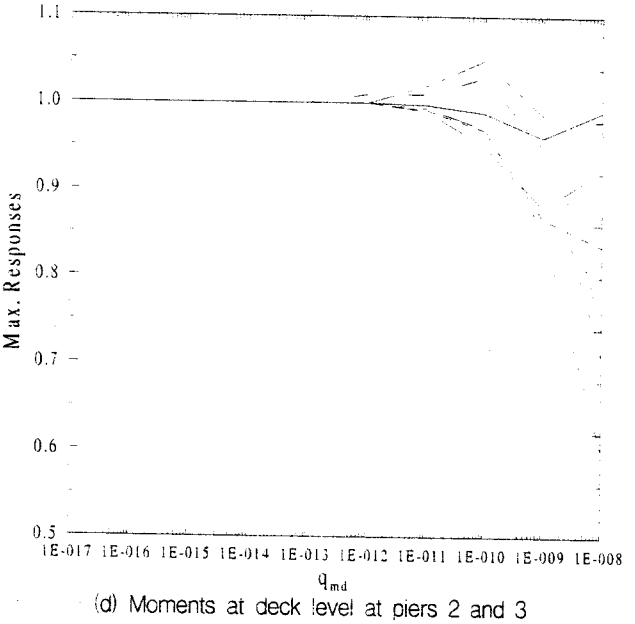

(d) Moments at deck level at piers 2 and 3

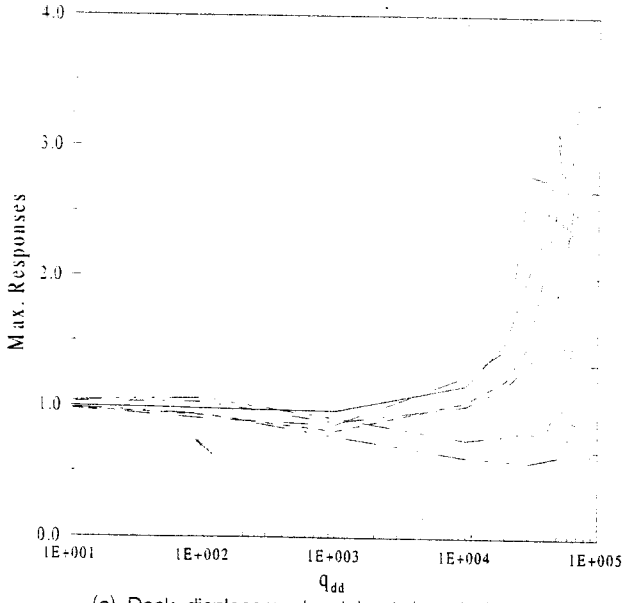

(e) Deck displacements at bent 1 and pier 4

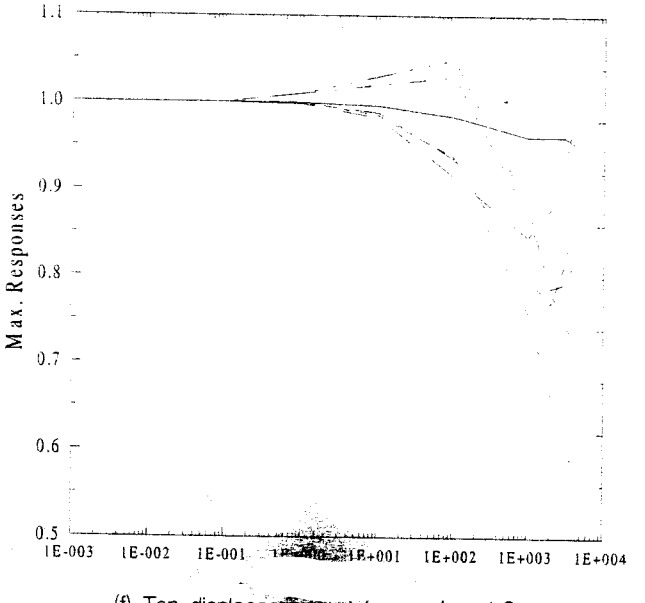

(f) Top displacements at towers 1 and 2

Fig. 6 Weighting parameters vs. max. responses for the hybrid control system

Table 3 Evaluation criteria for the 1940 El Centro NS earthquake

Criterion	Dyke et al.[7]	Passive Control	Active Control	Hybrid Control	Active/Hybrid
J_1 - peak base shear	0.3868	0.3976	0.2713	0.2642	1.0269
J_2 - peak shear at deck level	1.0681	1.1846	0.7899	0.7227	1.0930
J_3 - peak overturning mom.	0.2944	0.3054	0.2545	0.2298	1.1075
J_4 - peak mom. at deck level	0.6252	0.6077	0.4597	0.3828	1.2009
J_5 - peak dev. of cable tension	0.1861	0.2077	0.1474	0.1462	1.0082
J_6 - peak deck displacement	1.2006	1.4250	1.0059	0.7461	1.3482
J_7 - normed base shear	0.2257	0.2304	0.2001	0.1978	1.0116
J_8 - normed shear at deck level	1.1778	1.0909	0.7164	0.6933	1.0333
J_9 - normed overturning mom.	0.2665	0.2473	0.2010	0.1882	1.0680
J_{10} - normed mom. at deck level	0.8813	0.7128	0.5122	0.4953	1.0341
J_{11} - normed dev. of cable tension	2.2968e-2	2.2327e-2	1.6176e-2	1.8215e-2	0.8881
J_{12} - peak control force	1.5887e-3	1.3436e-3	1.9608e-3	LRB+HA : 2.6438e-3 LRB : 9.2908e-4 HA : 1.9608e-3	0.7417
J_{13} - peak stroke	0.7883	0.9356	0.6604	0.4899	1.3480
J_{14} - peak power	2.7011e-3	-	4.5696e-3	3.3152e-3	1.3784
J_{15} - peak total power	4.2871e-4	-	7.2528e-4	7.1034e-4	1.0210
J_{16} - no. of control devices	24	24	24	LRB+HA : 24+24	0.5000
J_{17} - no. of sensors	9	-	9	9	1.0000
J_{18} - no. of resources	30	-	30	30	1.0000

Table 4 Evaluation criteria for the 1985 Mexico City earthquake

Criterion	Dyke et al.[7]	Passive Control	Active Control	Hybrid Control	Active/Hybrid
J_1 - peak base shear	0.4582	0.5459	0.5071	0.4854	1.0447
J_2 - peak shear at deck level	1.3693	1.1097	0.9095	0.9270	0.9811
J_3 - peak overturning mom.	0.5836	0.6188	0.4485	0.4471	1.0031
J_4 - peak mom. at deck level	0.6140	0.4468	0.4154	0.3521	1.1798
J_5 - peak dev. of cable tension	7.7483e-2	4.8766e-2	4.4979e-2	4.6071e-2	0.9763
J_6 - peak deck displacement	2.3317	2.0197	1.6661	1.0797	1.5431
J_7 - normed base shear	0.3983	0.4211	0.3755	0.3723	1.0086
J_8 - normed shear at deck level	1.2118	0.9634	0.7700	0.7315	1.0526
J_9 - normed overturning mom.	0.4192	0.3989	0.3563	0.3336	1.0680
J_{10} - normed mom. at deck level	1.1067	0.6536	0.6912	0.5246	1.3176
J_{11} - normed dev. of cable tension	1.0276e-2	5.1805e-3	6.2671e-3	6.3367e-3	0.9890
J_{12} - peak control force	5.7440e-4	7.7631e-4	1.2201e-3	LRB+HA : 1.0851e-3 LRB : 6.4325e-4 HA : 7.5552e-4	1.1244
J_{13} - peak stroke	1.1742	1.0171	0.8390	0.5473	1.5330
J_{14} - peak power	1.7523e-3	-	2.6195e-3	1.0937e-3	2.3951
J_{15} - peak total power	2.3343e-4	-	3.4895e-4	1.9669e-4	1.7741
J_{16} - no. of control devices	24	24	24	LRB+HA : 24+24	0.5000
J_{17} - no. of sensors	9	-	9	9	1.0000
J_{18} - no. of resources	30	-	30	30	1.0000

requirements presented Dyke et al.[7] are 1000kN, 0.2m, and 1m/sec. As seen from Table 7, all the three maximum responses satisfy the actuator requirements in the active and hybrid control cases and the values of the hybrid control system is smaller than the active control system.

5. Conclusions

In this paper, a hybrid control strategy, which is composed of a passive control system to reduce the earthquake-induced forces in the structure and an active control system to further

Table 5 Evaluation criteria for the 1990 Gebze earthquake

Criterion	Dyke et al.[7]	Passive Control	Active Control	Hybrid Control	Active/Hybrid
J_1 - peak base shear	0.4540	0.4230	0.4139	0.3791	1.0918
J_2 - peak shear at deck level	1.3784	1.4616	1.1576	0.9360	1.2368
J_3 - peak overturning mom.	0.4434	0.5012	0.3419	0.2848	1.2005
J_4 - peak mom. at deck level	1.2246	1.2656	0.8792	0.6719	1.3085
J_5 - peak dev. of cable tension	0.1481	0.1598	9.0146e-2	9.5259e-2	0.9463
J_6 - peak deck displacement	3.5640	3.8289	1.8023	1.6629	1.0838
J_7 - normed base shear	0.3231	0.3340	0.2951	0.2773	1.0642
J_8 - normed shear at deck level	1.4271	1.5502	0.9510	0.9169	1.0372
J_9 - normed overturning mom.	0.4552	0.4815	0.3507	0.3240	1.0824
J_{10} - normed mom. at deck level	1.4569	1.4429	0.7618	0.7799	0.9768
J_{11} - normed dev. of cable tension	1.7052e-2	1.7129e-2	8.9002e-3	1.0398e-2	0.8560
J_{12} - peak control force	1.7145e-3	2.1611e-3	1.9608e-3	LRB+HA : 2.4626e-3 LRB : 1.2246e-3 HA : 1.7824e-3	0.7962
J_{13} - peak stroke	1.9540	2.0993	0.9886	0.9118	1.0842
J_{14} - peak power	7.3689e-3	-	9.3311e-3	6.6678e-3	1.3994
J_{15} - peak total power	6.9492e-4	-	8.7997e-4	8.4888e-4	1.0366
J_{16} - no. of control devices	24	24	24	LRB+HA : 24+24	0.5000
J_{17} - no. of sensors	9	-	9	9	1.0000
J_{18} - no. of resources	30	-	30	30	1.0000

Table 6 Maximum evaluation criteria for all the three earthquakes

Criterion	Dyke et al.[7]	Passive Control	Active Control	Hybrid Control	He et al.[17]
J_1 - peak base shear	0.4582	0.5459	0.5071	0.4854	0.4856
J_2 - peak shear at deck level	1.3784	1.4616	1.1576	0.9360	1.3536
J_3 - peak overturning mom.	0.5836	0.6188	0.4485	0.4471	0.5539
J_4 - peak mom. at deck level	1.2246	1.2656	0.8792	0.6719	1.2199
J_5 - peak dev. of cable tension	0.1861	0.2077	0.1474	0.1462	0.2176
J_6 - peak deck displacement	3.5640	3.8289	1.8023	1.6629	2.8227
J_7 - normed base shear	0.3983	0.4211	0.3755	0.3723	0.4083
J_8 - normed shear at deck level	1.4271	1.5502	0.9510	0.9169	1.4231
J_9 - normed overturning mom.	0.4552	0.4815	0.3563	0.3336	0.4588
J_{10} - normed mom. at deck level	1.4569	1.4429	0.7618	0.7799	1.5085
J_{11} - normed dev. of cable tension	2.2968e-2	2.2327e-2	1.6176e-2	1.8215e-2	0.0262
J_{12} - peak control force	1.7145e-3	2.1611e-3	1.9608e-3	LRB+HA : 2.6438e-3 LRB : 1.2246e-3 HA : 1.9608e-3	0.0125
J_{13} - peak stroke	1.9540	2.0993	0.9886	0.9118	-
J_{14} - peak power	7.3689e-3	-	9.3311e-3	6.6678e-3	-
J_{15} - peak total power	6.9492e-4	-	8.7997e-4	8.4888e-4	-
J_{16} - no. of control devices	24	24	24	LRB+HA : 24+24	-
J_{17} - no. of sensors	9	-	9	9	-
J_{18} - no. of resources	30	-	30	30	-

reduce the bridge responses, especially deck displacements, has been proposed by investigating the ASCE first generation benchmark control problem for seismic responses of cable-stayed bridges. The proposed control design uses conventional base isolation devices such as LRBs for the passive control part. The Bouc-Wen model is used to simulate the nonlinear behavior of these devices. Ideal hydraulic actuators are used for active control part and an H_2/LQG control algorithm

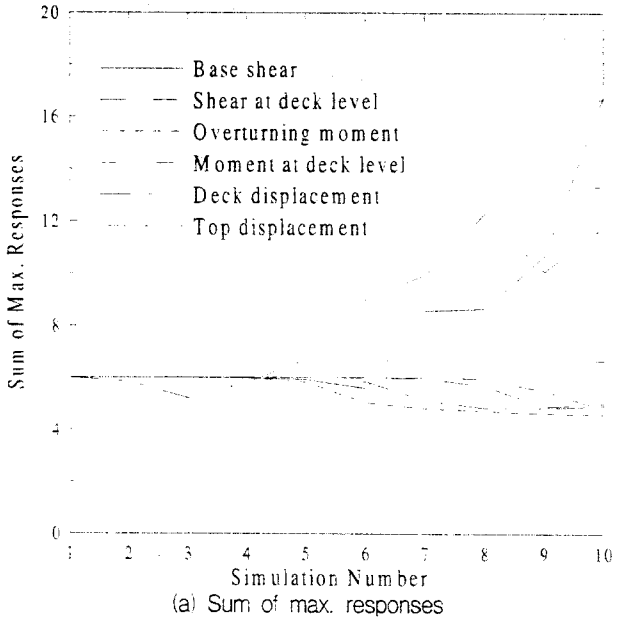

(a) Sum of max. responses

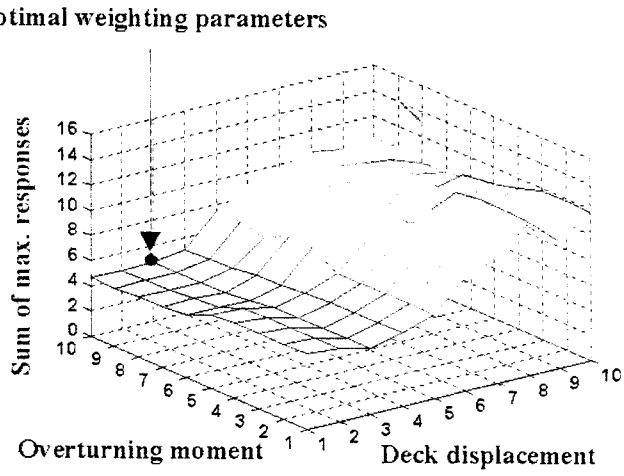

(b) Three dimensional analysis for the selected two weighting parameters

Fig. 7 Selection of appropriate optimal weighting parameters for the hybrid control system

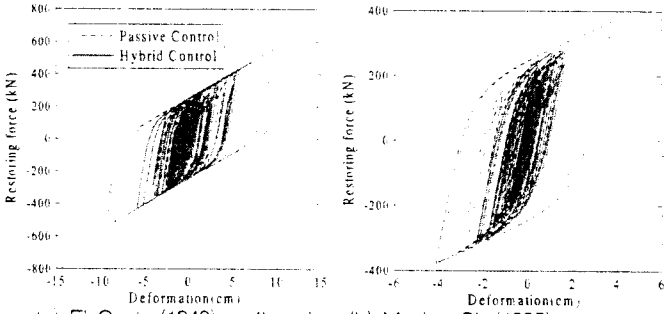

(a) El Centro(1940) earthquake (b) Mexico City(1985) earthquake

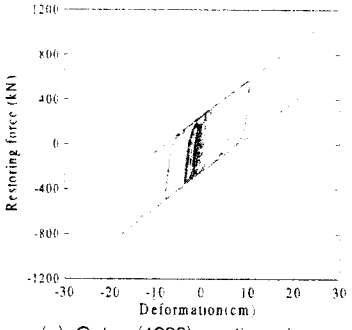

(c) Gebze(1990) earthquake

Fig. 8 Restoring force of LRB at pier 2

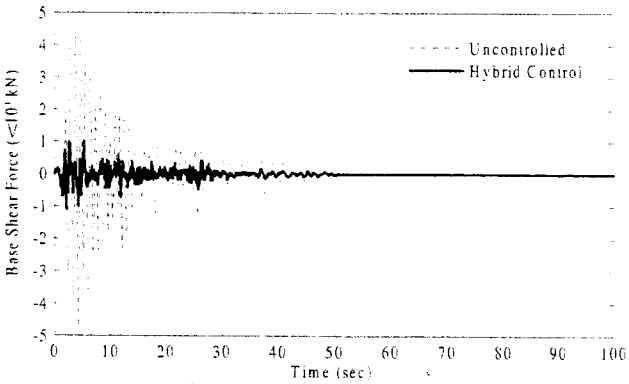

(a) El Centro(194) earthquake

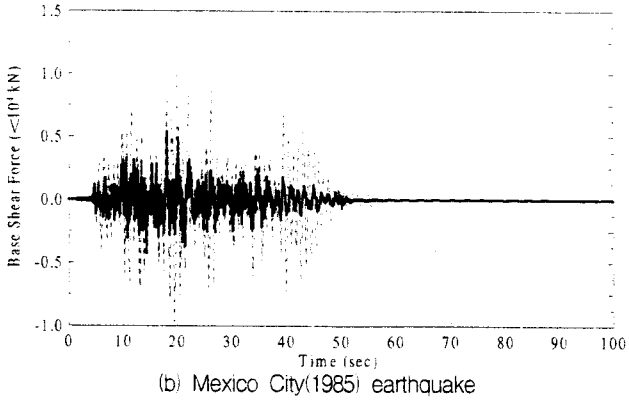

(b) Mexico City(1985) earthquake

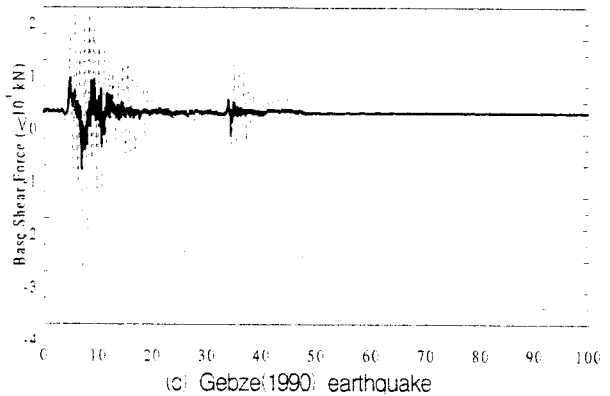

(c) Gebze(1990) earthquake

Fig. 9 Uncontrolled and hybrid controlled base shear force record at pier 2

Table 7 Actuator requirements for control strategies

Earthquake	Max.	Dyke et al.[7]	Active Control	Hybrid Control
1940 El Centro NS	Force(kN)	810.26	1000	1000
	Stroke(m)	0.1172	0.0982	0.0728
	Vel. (m/s)	0.6846	0.5499	0.5323
1985 Mexico City	Force(kN)	292.94	622.23	385.31
	Stroke(m)	0.0567	0.0405	0.0263
	Vel. (m/s)	0.3243	0.2374	0.2043
1990 Gebze NS	Force(kN)	874.41	1000	909.03
	Stroke(m)	0.2563	0.1297	0.1196
	Vel. (m/s)	0.5620	0.4157	0.4223